ACS Catalysis

Research Article

pubs.acs.org/acscatalysis

Trends in Electrochemical Stability of Transition Metal Carbides and Their Potential Use As Supports for Low-Cost Electrocatalysts

Yannick C. Kimmel,[†] Xiaoge Xu,[‡] Weiting Yu,[‡] Xiaodong Yang,[§] and Jingguang G. Chen*[,‡]

[†]Department of Chemical & Biomolecular Engineering, University of Delaware, Newark, Delaware 19716, United States

[‡]Department of Chemical Engineering, Columbia University, New York, New York 10027, United States

[§]State Key Laboratory for Mechanical Behavior of Materials, Xi'an Jiaotong University, Xi'an, Shaanxi 710049, People's Republic of China

ABSTRACT: Early transition metal carbides (TMCs) can be used as supports for platinum-group metals as low-cost electrocatalysts. The determination of electrochemical stability of TMCs is important to identify their potential use in electrochemical and photoelectrochemical applications. Various TMC thin films were synthesized and characterized with X-ray diffraction and photoelectron spectroscopy. Chronopotentiometric-titration measurements were used to map the stability regions of the TMC thin films over a wide pH range. The stability of the TMC thin films was correlated to the oxygen binding energy of the parent metal. All of the TMCs studied are stable for hydrogen evolution/oxidation; most are stable for alcohol oxidation, and titanium, tantalum, and zirconium carbides are stable for oxygen evolution/reduction reactions.

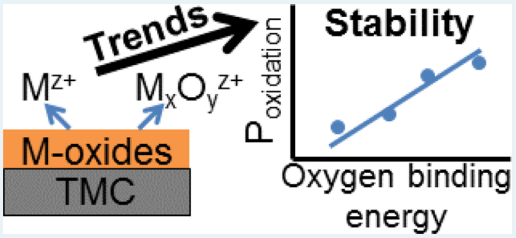

KEYWORDS: *transition metal carbide (TMC), electrocatalysts, stability, X-ray photoelectron spectroscopy, DFT, chronopotentiometry, X-ray diffraction*

1. INTRODUCTION

Fuel cells and electrolyzers typically require the use of significant amounts of precious metals, such as platinum (Pt), palladium (Pd), and iridium (Ir), which can greatly increase the cost of these devices. It has been established that early transition (groups 4–6) metal carbides (TMCs) often share similar electronic and catalytic properties with the Pt-group metals[1,2] and can be used as supports to reduce the overall loading of the precious metals.[3] The parent metals of TMCs are orders of magnitude more abundant in the earth's crust and less expensive than Pt-group metals. Economically, any replacement of Pt with TMCs can result in a great reduction in the catalyst cost.[4,5] These properties of TMCs make them ideal supports for Pt-group metals. Previous work in our research group has found that an ultralow loading of one monolayer (ML) of Pt can be stable on several TMC supports while behaving as active as bulk Pt for the hydrogen evolution reaction (HER).[5,6]

Tungsten carbide (WC) has been studied extensively as both a stand-alone electrocatalyst and as a support for Pt-group metals for the HER,[4,7−9] hydrogen oxidation reaction (HOR),[9,10] methanol oxidation reaction,[11] and oxygen reduction reaction (ORR).[12,13] However, the promising properties of other TMCs can also be advantageous; for example, the low synthesis temperature of titanium carbide (TiC) results in high surface area powders being available for purchase.[14] Pt-group metals supported on vanadium (VC) and tantalum (TaC) carbides have been shown to have synergistic effects for the ORR,[15,16] and zirconium carbide (ZrC) was shown to be a good support for HOR.[17] There are ongoing efforts to synthesize TMC particles that have surface areas high enough to be used as powder supports.[18−20]

An electrocatalyst or support must be stable under a given range of pH and potential values to be useful. For pure metals, the stability information can be typically obtained in widely available Pourbaix diagrams. These diagrams do not exist for TMCs, and therefore, there is need to explore the stability of TMCs under a large range of electrochemical conditions. Pseudo-Pourbaix diagrams[21,22] can be used to identify three regions of electrochemical stability of the TMCs by use of chronopotentiometric (CP)-titration measurements: immunity, passivation, and sustained oxidation from an applied potential. In CP-titration measurements, the open circuit potential (OCP) is recorded as a function of pH, and this potential represents the balance between the overall reduction and oxidation reactions. Above the OCP, the TMC begins to oxidize and may form a passivation layer that prevents further oxidization, allowing the surface to remain stable. If the applied potential is high enough, the passivation layer breaks down and the TMC undergoes oxidization and becomes unstable. In this work, the potential at a current density of +0.1 mA cm^{-2} was chosen as the onset of sustained oxidization to identify regions of stability of TMCs for various electrochemical applications. These pseudo-Pourbaix diagrams provide guidance on the operational pH and applied potential for a TMC to remain in

Received: February 11, 2014
Revised: March 31, 2014
Published: April 7, 2014

   dx.doi.org/10.1021/cs500182h | ACS Catal. 2014, 4, 1558−1562

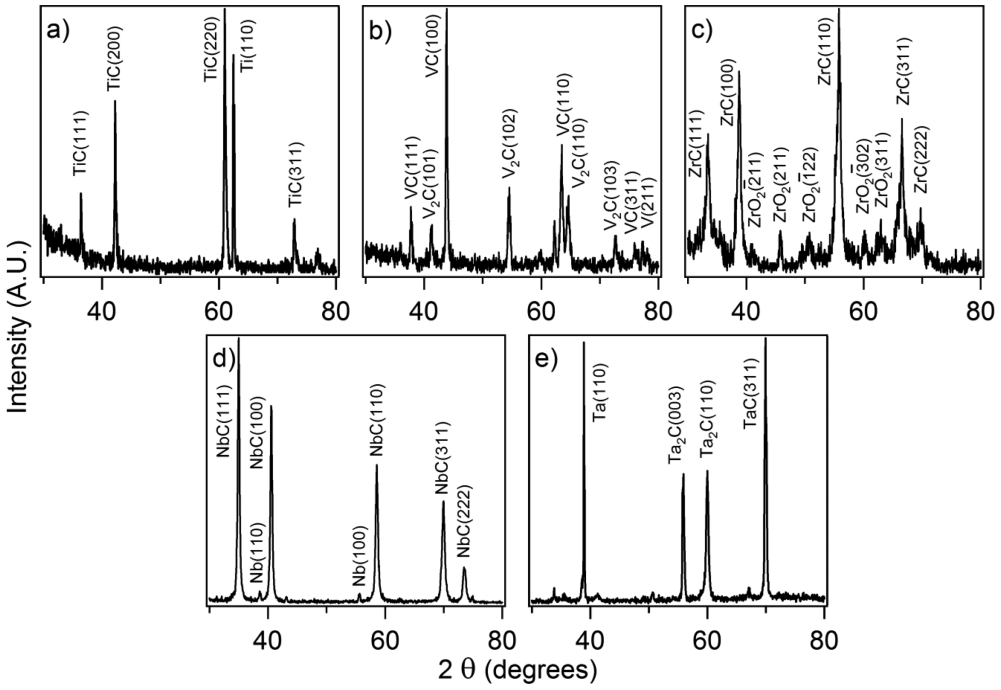

Figure 1. XRD patterns of (a) TiC, (b) VC, (c) ZrC, (d) NbC, and (e) TaC films.

the immunity or passivation regions and avoid sustained oxidization.

In this current paper, TiC, VC, ZrC, niobium carbide (NbC), and TaC films were synthesized and characterized with X-ray diffraction (XRD) and X-ray photoelectron spectroscopy (XPS). CP-titration measurements were performed on these TMC films to determine the stability under a wide range of pH and potential values. These results, along with previous CP titration data on WC and Mo_2C, were used to identify regions where TMCs will be stable as electrocatalysts or supports for common electrochemical energy conversion applications. Density functional theory (DFT) was used to identify a trend for the stability and resistance toward electrooxidation of the various TMCs. The systematic examination of the TMC electrochemical stability can be helpful for the identification of TMCs in electrocatalytic and photoelectrocatalytic applications.

2. EXPERIMENTAL SECTION

2.1. TMC Synthesis. Niobium foil (0.127 mm thick, 99.97% excluding Ta), vanadium foil (0.075 mm thick, 99.8%), titanium foil (0.127 mm thick, 99.99+%), tantalum foil (0.25 mm thick, annealed 99.95%), and zirconium foil (0.127 mm thick, annealed 99.5%) were purchased from Alfa Aesar and rinsed with acetone and then 0.3 M sodium hydroxide (NaOH) before being carburized. All metal foils except Ti were carburized in a tube furnace with a flow rate of 122 cm^3 min^{-1} of hydrogen (H_2) and 32.6 cm^3 min^{-1} of methane (CH_4) at 1273 K for 1 h before being cooled to 1123 at 3.3 K min^{-1}, at this point, the CH_4 was turned off and the temperature was held for 15 min before the furnace was turned off to help remove excess surface carbon.[23] After the films were cooled to room temperature, the H_2 flow was turned off, and a gas mixture of 1% oxygen/99% nitrogen was flown over the films to passivate for 1 h before exposure to the atmosphere. Ti foil was carburized with a flow rate of 108 cm^3 min^{-1} for H_2 and 46 cm^3 min^{-1} for CH_4 at 1373 K for 4 h. After the TiC film was passivated in a manner identical to that for the other TMC films, the excess surface carbon was peeled off the TiC film.

2.2. Characterization. Scintag X2 advanced diffraction system with a Cu Kα X-ray source was used to measure symmetric XRD with a count time of 2 s and step size of 0.05°. A Phi 1600 XPS system with an Al X-ray source and hemispherical analyzer was used for XPS measurements.

2.3. Electrochemical Methods. The TMC films were stored under vacuum before and after electrochemistry to prevent oxidation from atmosphere and were dipped in 0.3 M NaOH to remove surface metal oxides immediately before electrochemical measurements. A new TMC film was used for every CP-titration measurement. CP-titration measurements were conducted using a three-electrode set-up with a Pt gauze counter electrode and a double-junction saturated calomel reference electrode (Pine Research Instrumentation), and a Princeton Applied Research VersaSTAT 4 or VersaSTAT 3F was used as a potentiostat/galvanostat. The electrolyte consisted of a nitrogen-saturated solution of 0.1 M phosphoric acid buffer (Fisher Chemical, 85% certified ACS), 0.1 M sodium sulfate (Fisher Chemical, anhydrous certified ACS) to ensure that both sodium and sulfate ions were present, and various amounts of concentrated sulfuric acid (Fisher Chemical, TraceMetal grade) and concentrated NaOH (Fisher Chemical, certified ACS) to achieved the desirable pH values. The CP measurements were taken at a pH value starting at ~0.5 and ending at ~13. The pH was measured continuously with an Accumet AP61 pH meter and titrated with concentrated NaOH. The potential was allowed to reach steady state before the pH was changed. For more details on the CP-titration measurements, see the literature.[21,22]

2.4. Theoretical Methods. All DFT calculations were performed with the Vienna Ab Initio Simulation Package (VASP).[24−27] The PW 91 functional[28] was used in the generalized gradient approximation (GGA)[29] calculation, and a kinetic cutoff energy of 396 eV was chosen for the plane wave truncation. The most close-packed surfaces of Mo(110),

dx.doi.org/10.1021/cs500182h | ACS Catal. 2014, 4, 1558−1562

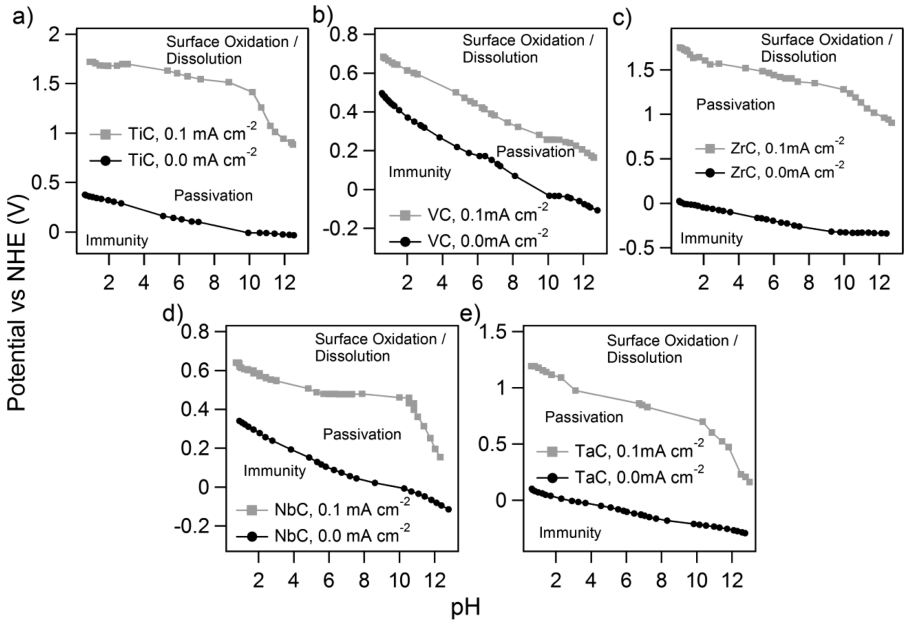

Figure 2. Chronopotentiometric (CP)-titration curves for (a) TiC, (b) VC, (c) ZrC, (d) NbC, and (e) TaC. The uncertainty associated with the average variation in steady state potential is smaller than the size of the data points shown.

Nb(110), Ta(110), V(110), W(110), Ti(0001), and Zr(0001) were used for the calculations. All calculations were performed using a periodic 3 × 3 unit cell with a 3 × 3 × 1 Monkhorst–Pack k-point grid. Each surface was modeled by adding six equivalent layers of vacuum onto four metal layers, in which the two bottom layers were frozen, while the top two layers were allowed to relax to reach the lowest energy configuration.

In oxygen binding energy (OBE) calculations, oxygen was placed on the atop, bridge, and 3-fold sites to determine the most stable binding configuration. A coverage of 1/9 was used for each OBE calculation. The OBE on each surface was calculated by subtracting the energies of the bare surface and an oxygen atom from the total energy of the slab plus the adsorbed oxygen atom.

3. RESULTS AND DISCUSSION

3.1. Characterization of TMC films. XRD was used to determine the structure of the TMC films (Figure 1). The labeled crystal facets were matched from literature for Ti [ICDD 00-044-1294], TiC [ICDD 00-032-1383], V [00-022-1058], V_2C [01-071-6320],VC [ICDD 01-073-0476], ZrC [ICDD 00-035-0784], ZrO_2 [ICDD 00-036-0420], Nb [ICDD 00-034-0370], NbC [ICDD 00-010-0181], Ta [ICDD 00-004-0788], Ta_2C [ICDD 01-071-2677], and TaC [ICDD 00-035-0801]. Figure 1d indicates that NbC films are phase-pure with no other metallic or carbidic phases present. The XRD patterns for VC, TiC, and TaC show mixed metallic and carbidic phases. Similar work on WC film[30] synthesized in an identical manner found that WC-phase is present near the surface, whereas the W_2C and W phases are present in the bulk. This would suggest that fully carburized V, Ti, and Ta would also be present near the surface. There is a mixture of Zr carbide and oxide peaks in the ZrC film XRD, which indicates that the film is not fully carburized.

3.2. CP-Titration Measurements. CP-titration measurements were conducted at two current densities and represented the regions of stability (Figure 2). The first current density was at 0.0 mA cm^{-2}, which approximates the boundary between immunity and passivation, and the second current density was at +0.1 mA cm^{-2} which represents the boundary between passivation and TMC dissolution. Generally, the OCP decreases in a linear fashion as the pH increases. This decrease is mostly due to the pH dependence of the reversible hydrogen adsorption/desorption potential at room temperature (−59 mV/pH unit),[22] but can also be influenced by other reduction/oxidation reactions. At low to moderate pH, the +0.1 mA cm^{-2} CP curves for the ZrC, NbC, and TaC films decrease at a linear rate that has been previously attributed to the formation of solid oxide product.[22] This is in contrast to previous CP-titration measurements for WC that found that WC possesses a substantially decreased region of passivation at neutral and alkaline pH values.[21] The +0.1 mA cm^{-2} CP potential decreases rapidly at very high pH (>10) for TiC, NbC, and TaC, and this large negative change has been corresponded to dissolution of metal oxides into solution.[22] Previous work[31] found that TiC, when subjected to galvanostatic corrosion under acidic conditions, exhibits a plateau at two different potentials: the first one is temporary and is due to the passivation of TiC film (partially reduced Ti oxide), whereas the potential at steady state reflects the dissolution of a solid oxide. The potential of the Ti solid oxide dissolution from this prior study is very close to that of the potential at +0.1 mA cm^{-2} (Figure 2a) under acidic conditions, so the CP could be more representative of Ti oxide than Ti carbide. Generally, the CP-titration measurements show that TMCs have higher stability than predicted for the parent metals from Pourbaix diagrams.[32] The TMCs also show high stability at low pH, whereas common nonprecious, catalytically active metals (e.g., Ni, Cu, and Fe) are known to be unstable under acidic conditions.[33] Therefore, TMCs could be useful as stable materials for acidic electrocatalysis. It is important to note that the kinetically limited CP-titration measurements are approximating the thermodynamic stability in a Pourbaix diagram, so there are external factors that may shift the TMC regions of stability and also do not take into account active corrosion that does not require an external applied potential.

dx.doi.org/10.1021/cs500182h | ACS Catal. 2014, 4, 1558–1562

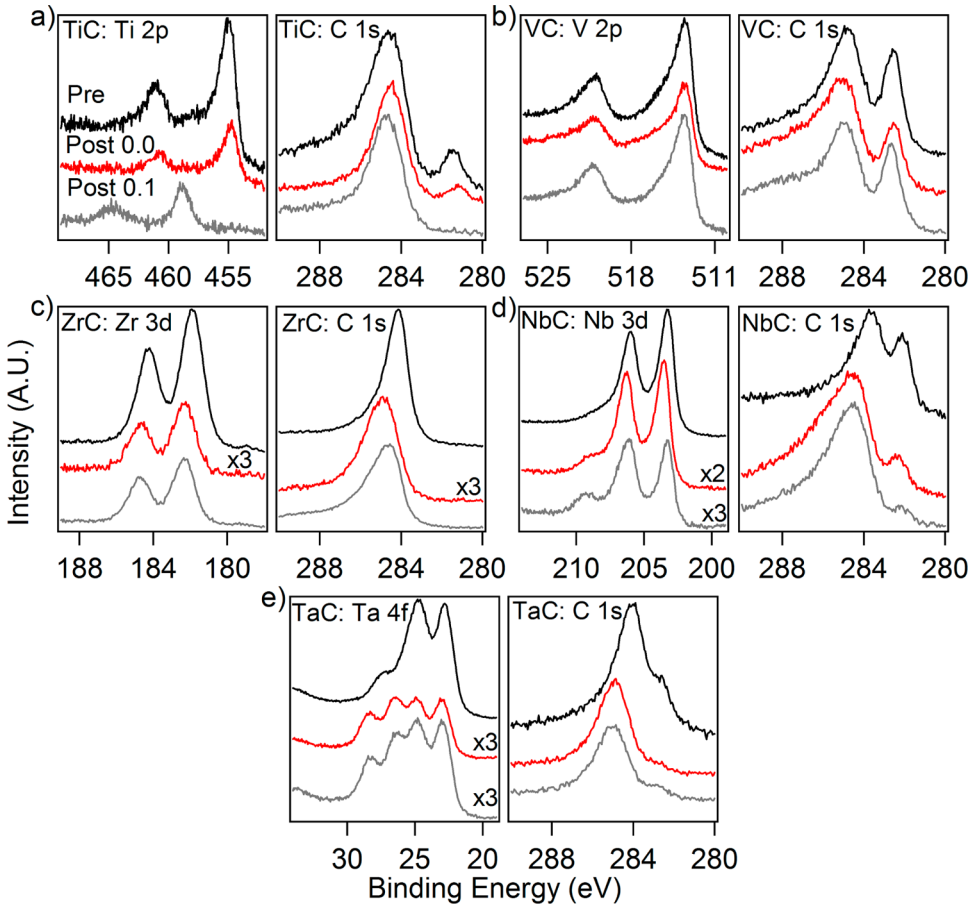

Figure 3. XPS spectra of (a) TiC, (b) VC, (c) ZrC, (d) NbC, and (e) TaC film pre (black line), post 0.0 mA cm^{-2} (red line), and post +0.1 mA cm^{-2} (gray line) CP-titration measurement. A new TMC film was used for each CP-titration measurement.

3.3. Surface Characterization Pre and Post CP Measurements. To investigate the oxidation state near the surface region of the TMC films, XPS measurements were performed before and after the CP-titration measurements (Figure 3). The metal 2p, 3d, or 4f XPS regions for TiC, VC, NbC, and TaC films before the CP experiment show that the metallic components are present in their carbidic form, and there are shoulders present at higher BE indicating that a small amount of metal oxide is also present, as is expected for passivated surfaces. The C 1s region of these TMC films also confirms the presence of a carbidic C (peak location <284.8 eV) and a graphitic C (peak location ~284.8 eV). The XPS spectra of VC, NbC, and TaC films show that there is either no metal oxide (VC) or a small amount of metal oxide (NbC and TaC) after the CP measurements. XPS results of the ZrC film (Figure 3c) indicate that before CP measurement, the metal near the surface is fully oxidized, and the ZrC film does not passivate well, so measurements may reflect the potential of oxidation for Zr oxide. The TiC film is carbidic near the surface before the CP measurement, but the XPS afterward shows that the TiC surface is completely oxidized, suggesting that the 0.1 mA cm^{-2} CP measurements for TiC could represent the oxidation potential of titanium oxide rather than TiC.

3.4. Trends in TMC Stability. The CP-titration results are organized under two regions of interest in electrocatalysis in Figure 4—acidic (pH = 1) or alkaline (pH = 12; except Mo_2C for which pH = 11) conditions—and the potentials are reported vs RHE to allow for easy comparison by eliminating

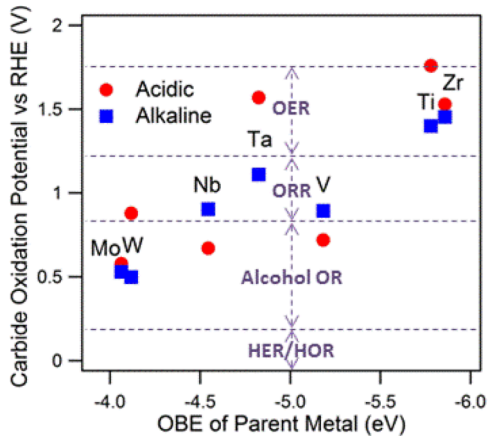

Figure 4. Oxidation potential of metal carbide as a function of DFT-calculated oxygen binding energy (OBE) of the parent metal. The oxidation potentials for WC and Mo_2C were taken from the literature.[22] The dashed lines superimposed over the data represent the general operational potentials of common electrochemical reactions.

the effects of pH. The potential that the carbide will sustain oxidation (+0.1 mA cm^{-2}) is plotted as a function of DFT-calculated OBE of the parent metal. There is a general correlation between strong OBE and high potential for the onset of oxidation for the TMC, with the correlation being more obvious for alkaline than acidic conditions. The better

dx.doi.org/10.1021/cs500182h | ACS Catal. 2014, 4, 1558−1562

correlation under alkaline conditions could be because of the similarities between hydroxide present in solution and oxygen adsorbed on the TMC surfaces. One possible reason that a higher OBE value corresponds to a more stable TMC is because the TMC is passivated (as identified in the XPS results), which results in a small amount of oxidized metal protecting the TMC from further oxidation. TiC and ZrC have a much stronger OBE than the other metals in the current study, which could explain why those two carbides show complete metal oxidation in the XPS after the +0.1 mA cm^{-2} CP measurements. Ta, W, Ti, and Zr carbide show stability under acidic conditions; Ti, Zr, Ta, V, and Nb carbide show stability under alkaline conditions. The general operational potentials of common electrochemical reactions (oxygen evolution, oxygen reduction, alcohol oxidation, hydrogen oxidation, and hydrogen evolution) are superimposed over the data to allow identification of potential applications of TMCs. Generally, all of the TMCs are stable for HER/HOR, and most are stable for alcohol oxidation. TaC, TiC, and ZrC also show stability for ORR or OER.

4. CONCLUSIONS

TMCs are promising supports for Pt-group metal electrocatalysts. This work identified the regions of stability for TMCs as a guide for their selection in various electrochemical applications. Overall, the electrochemical stability was correlated with the DFT-calculated OBE values. Specifically, ZrC, TiC, and TaC films exhibited the highest stability in both acidic and alkaline solutions.

AUTHOR INFORMATION

Corresponding Author

*Phone: +1 2128546166. Fax: +1 2128543054. E-mail: jgchen@columbia.edu.

Notes

The authors declare no competing financial interest.

ACKNOWLEDGMENTS

The authors acknowledge support from the Department of Energy, Office of Basic Energy Sciences (Grant No. DE-FG02-13ER16381). DFT calculations were supported by computational resources from the Center for Functional Nanomaterials at Brookhaven National Lab. The authors also thank Yeh-Chun Hsu for help with the preliminary CP-titration experiments and Prof. Daniel Esposito for useful discussions.

REFERENCES

(1) Ham, D. J.; Lee, J. S. *Energies* **2009**, *2* (4), 873−899.
(2) Hwu, H. H.; Chen, J. G. *Chem. Rev.* **2005**, *105* (1), 185−212.
(3) Kelly, T. G.; Chen, J. G. *Chem. Soc. Rev.* **2012**, *41* (24), 8021−8034.
(4) Esposito, D. V.; Chen, J. G. *Energy Environ. Sci.* **2011**, *4* (10), 3900−3912.
(5) Esposito, D. V.; Hunt, S. T.; Stottlemyer, A. L.; Dobson, K. D.; McCandless, B. E.; Birkmire, R. W.; Chen, J. G. *Angew. Chem.-Int. Ed.* **2010**, *49* (51), 9859−9862.
(6) Kimmel, Y. C.; Yang, L.; Kelly, T. G.; Rykov, S. A.; Chen, J. G. *J. Catal.* **2014**, *312*, 216−220.
(7) Chen, W.-F.; Muckerman, J. T.; Fujita, E. *Chem. Commun.* **2013**, *49*, 8896−8909.
(8) Wirth, S.; Harnisch, F.; Weinmann, M.; Schröder, U. *Appl. Catal., B* **2012**, *126* (0), 225−230.
(9) Vasić, D. D.; Pašti, I. A.; Mentus, S. V. *Int. J. Hydrogen Energy* **2013**, *38* (12), 5009−5018.
(10) Hara, Y.; Minami, N.; Matsumoto, H.; Itagaki, H. *Appl. Catal., A* **2007**, *332* (2), 289−296.
(11) Weigert, E. C.; Stottlemyer, A. L.; Zellner, M. B.; Chen, J. G. *J. Phys. Chem. C* **2007**, *111* (40), 14617−14620.
(12) Hsu, I. J.; Hansgen, D. A.; McCandless, B. E.; Willis, B. G.; Chen, J. G. *J. Phys. Chem. C* **2011**, *115* (9), 3709−3715.
(13) Hsu, I. J.; Kimmel, Y. C.; Dai, Y.; Chen, S. L.; Chen, J. G. *J. Power Sources* **2012**, *199*, 46−52.
(14) AlfaAesar; *Titanium Carbide, Product No. 44922*; www.alfa.com; accessed 12/2012.
(15) Hu, Z.; Chen, C.; Meng, H.; Wang, R.; Shen, P. K.; Fu, H. *Electrochem. Commun.* **2011**, *13* (8), 763−765.
(16) Polonský, J.; Petrushina, I. M.; Christensen, E.; Bouzek, K.; Prag, C. B.; Andersen, J. E. T.; Bjerrum, N. J. *Int. J. Hydrogen Energy* **2012**, *37* (3), 2173−2181.
(17) Horigome, M.; Kobayashi, K.; Suzuki, T. M. *Int. J. Hydrogen Energy* **2007**, *32* (3), 365−370.
(18) Tao, X.; Li, Y.; Du, J.; Xia, Y.; Yang, Y.; Huang, H.; Gan, Y.; Zhang, W.; Li, X. *J. Mater. Chem.* **2011**, *21* (25), 9095−9102.
(19) Li, P. G.; Lei, M.; Sun, Z. B.; Cao, L. Z.; Guo, Y. F.; Guo, X.; Tang, W. H. *J. Alloys Compd.* **2007**, *430* (1−2), 237−240.
(20) Yan, Z.; Cai, M.; Shen, P. K. *J. Mater. Chem.* **2011**, *21* (47), 19166−19170.
(21) Weidman, M. C.; Esposito, D. V.; Hsu, I. J.; Chen, J. G. *J. Electrochem. Soc.* **2010**, *157* (12), F179−F188.
(22) Weidman, M. C.; Esposito, D. V.; Hsu, Y. C.; Chen, J. G. *J. Power Sources* **2012**, *202*, 11−17.
(23) Kimmel, Y. C.; Esposito, D. V.; Birkmire, R. W.; Chen, J. G. *Int. J. Hydrogen Energy* **2012**, *37* (4), 3019−3024.
(24) Ammann, C. M.; Meehl, G. A.; Washington, W. M.; Zender, C. S. *Geophys. Res. Lett.* **2003**, *30* (12), 1657.
(25) Kresse, G.; Furthmuller, J. *Phys. Rev. B* **1996**, *54* (16), 11169−11186.
(26) Kresse, G.; Furthmuller, J. *Comput. Mater. Sci.* **1996**, *6* (1), 15−50.
(27) Kresse, G.; Hafner, J. *Phys. Rev. B* **1993**, *47* (1), 558−561.
(28) Perdew, J. P.; Chevary, J. A.; Vosko, S. H.; Jackson, K. A.; Pederson, M. R.; Singh, D. J.; Fiolhais, C. *Phys. Rev. B* **1992**, *46* (11), 6671−6687.
(29) Teter, M. P.; Payne, M. C.; Allan, D. C. *Phys. Rev. B* **1989**, *40* (18), 12255−12263.
(30) Esposito, D. V.; Dobson, K. D.; McCandless, B. E.; Birkmire, R. W.; Chen, J. G. *J. Electrochem. Soc.* **2009**, *156* (8), B962−B969.
(31) Cowling, R. D.; Hintermann, H. E. *J. Electrochem. Soc.* **1970**, *117* (11), 1447−1449.
(32) Liu, Y.; Kelly, T. G.; Chen, J. G.; Mustain, W. E. *ACS Catal.* **2013**, *3* (6), 1184−1194.
(33) Jones, D. A. *Principles and Prevention of Corrosion*, 2nd ed.; Prentice Hall: Upper Saddle River, NJ, 1996.